

Supporting Information: Hydroperoxyl radical and formic acid formation from common DNA stabilizers upon low energy electron attachment

*Anita Ribar, †, ‡ Stefan E. Huber, †, ¶ Malgorzata A. Śmiałek, *, §, || Katrin Tanzer, † Michael
Neustetter, † Robin Schürmann, ⊥ Ilko Bald, ⊥ and Stephan Denifl*, †*

†Institute for Ion Physics and Applied Physics and Center of Molecular Biosciences
Innsbruck, Leopold Franzens University of Innsbruck, Technikerstr. 25, 6020 Innsbruck
Austria,

‡Faculty of Mathematics, Physics and Informatics, Comenius University in Bratislava,
Mlynská dolina F2, 842 48 Bratislava, Slovakia

¶Institute for Basic Sciences in Engineering Science, Leopold Franzens University of
Innsbruck, Technikerstr. 13, 6020 Innsbruck, Austria,

§Department of Control and Power Engineering, Faculty of Ocean Engineering and Ship
Technology, Gdansk University of Technology, Gabriela Narutowicza 11/12, 80-233 Gdansk,
Poland,

||School/ of Physical Sciences, The Open University, Walton Hall, Milton Keynes MK7 6AA,
United Kingdom,

⊥Institute of Chemistry – Physical Chemistry, University of Potsdam, Karl-Liebknecht-Str.
24-25, D-14476 Potsdam, Germany

1) TRIS

1.1 Experimental:

In Figure S1 we present the experimentally determined anion efficiency curves of less abundant fragment anions formed upon dissociative electron attachment (DEA) to TRIS.

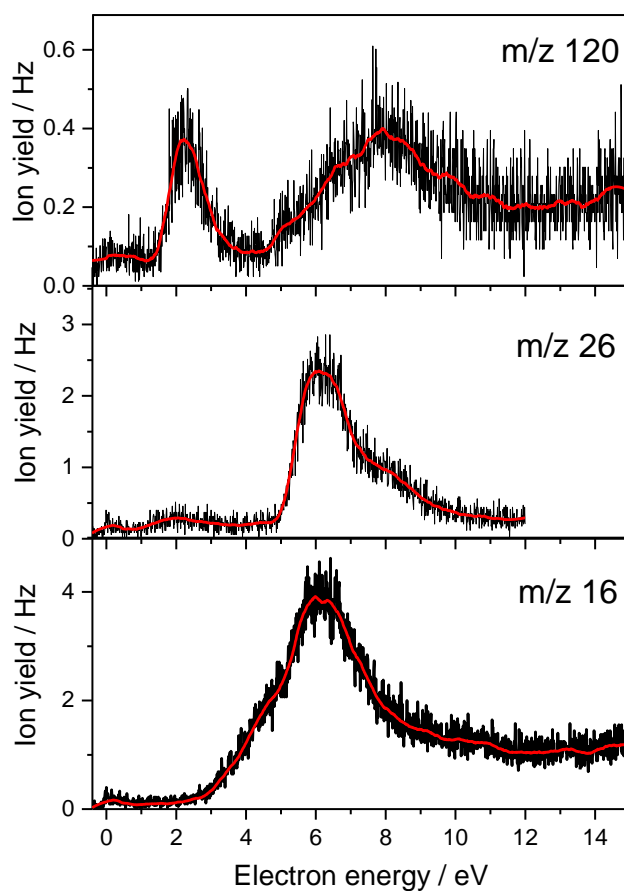


Figure S1. Measured anion efficiency curves for m/z 16, 26 and 120 formed upon DEA to TRIS.

1.2 Computational:

In Table S1 below, we supply the computed thermochemical reaction thresholds at room temperature (298.15 K) for all considered fragmentation reactions upon DEA to 2-amino-2-(hydroxymethyl)-1,3-propanediol (TRIS), see Fig. S2. The thresholds presented in Table S1 were determined by computing the Gibbs free energies of reactants, $E(R)$, and products, $E(P)$, and by calculating subsequently, the thermochemical reaction threshold, $E(P \rightarrow R) = E(P) - E(R)$. For the calculation of the Gibbs free energies the G4(MP2) extrapolation scheme was used. G4(MP2) is the most recent of the Gx extrapolation schemes developed by Curtiss and coworkers (1). The method yields an average deviation of about 0.05 eV from experiment for the 454 energies compiled in the G3/05 test set (1). All calculations were performed with the Gaussian 09 program (2).

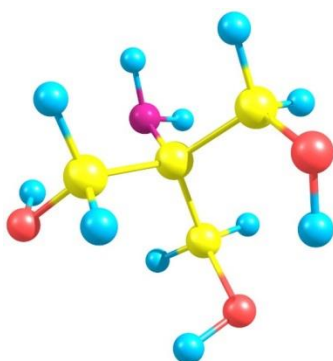


Figure S2: Structure of 2-amino-2-(hydroxymethyl)-1,3-propanediol (TRIS) as obtained at the B3LYP/6-31G(2df,p) level of theory, i.e. the level of theory used for geometry optimization in the composite G4(MP2) extrapolation scheme. Red: oxygen; purple: nitrogen; yellow: carbon; blue: hydrogen.

Table S1: Gibbs free reaction energies at 298.15 K for all considered fragmentation reactions upon DEA to TRIS.

Reaction pathway: $e^- + \text{TRIS} \rightarrow$	m/z	Reaction energy (eV)
$(\text{TRIS-H})^- + \text{H}$ (H from OH)	120	1.27
$(\text{TRIS-H})^- + \text{H}$ (H from CH_2)	120	1.27
$(\text{TRIS-H})^- + \text{H}$ (H from NH_2)	120	1.82
$(\text{TRIS-NH}_2)^- + \text{NH}_2^{\text{a}}$	105	1.78
$(\text{TRIS-OH})^- + \text{OH}$	104	1.13
$(\text{TRIS-O}_2\text{H})^- + \text{O}_2\text{H}^{\text{b}}$	88	2.99
$(\text{TRIS-O}_2\text{H-O})^- + \text{O}_2\text{H} + \text{O}^{\text{c}}$	72	8.26
$(\text{TRIS-OH-OH-OH})^- + \text{OH} + \text{OH} + \text{OH}$	70	7.95
$(\text{TRIS-OH-OH-OH})^- + \text{O}_2\text{H} + \text{H}_2\text{O}$	70	4.82
$(\text{TRIS-OH-OH-OH})^- + \text{O}_2\text{H}_2 + \text{OH}$	70	6.22
$(\text{TRIS-OH}) + \text{OH}^-$	17	1.63
$(\text{TRIS-OH-NH}_2) + \text{OH}^- + \text{NH}_2$	17	2.24
$(\text{TRIS-OH-OH-NH}) + \text{OH}^- + \text{OH} + \text{NH}$	17	5.46
$(\text{TRIS-OH-OH-OH}) + \text{OH}^- + \text{OH} + \text{OH}$	17	6.32
$(\text{TRIS-O}) + \text{O}^-$	16	2.35
$(\text{TRIS-NH}_2) + \text{NH}_2^-$	16	2.39
$(\text{TRIS-OH-NH}_2) + \text{OH} + \text{NH}_2^-$	16	3.31
$(\text{TRIS-OH-OH-NH}) + \text{OH} + \text{OH} + \text{NH}^-$	15	7.02
$(\text{TRIS-H}) + \text{H}^-$ (H from OH)	1	3.91
$(\text{TRIS-H}) + \text{H}^-$ (H from CH_2)	1	3.38
$(\text{TRIS-H}) + \text{H}^-$ (H from NH_2)	1	3.71

^a For m/z = 105 also the reaction channel leading to the formation of $(\text{TRIS-O})^-$ and O was considered. However, no stable valence bound anion could be identified for the fragment $(\text{TRIS-O})^-$.

^b For m/z = 88 also the reaction channel leading to the formation of $(\text{TRIS-OH-NH}_2)^-$, OH and NH_2 was considered. However, no stable valence bound anion could be identified for the fragment $(\text{TRIS-OH-NH}_2)^-$.

^c For m/z = 72 also the reaction channel leading to the formation of $(\text{TRIS-OH-OH-NH})^-$, 2 OH and NH was considered. However, no stable valence bound anion could be identified for the fragment $(\text{TRIS-OH-OH-NH})^-$.

2) EDTA and MIDA

2.1. Experimental:

In Figure S3 we present the experimentally determined anion efficiency curve of less abundant fragment anions formed upon dissociative electron attachment (DEA) to MIDA.

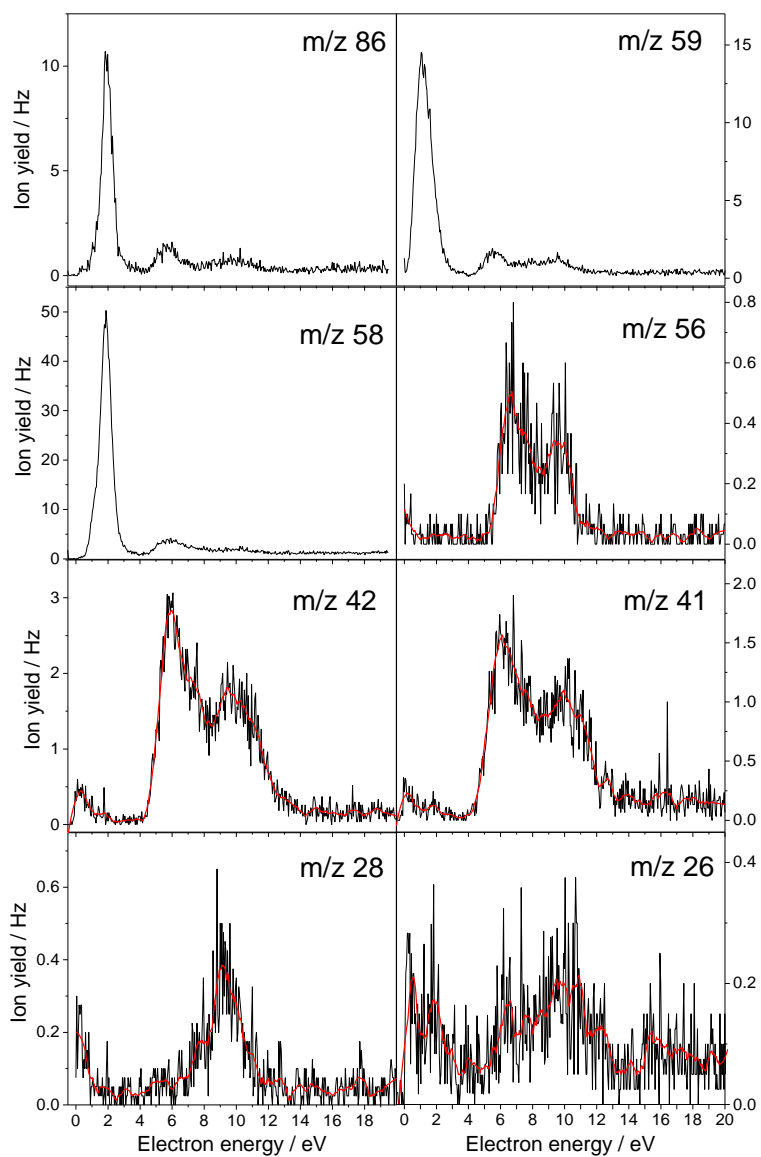


Figure S3: Anion efficiency curves for m/z 26, 28, 41, 42, 56, 58, 59 and 86 formed upon DEA to MIDA.

2.2. Computational

2.2.1. Introductory remarks to the calculations

As described in the main text, thermal decomposition of ethylenediaminetetraacetic acid (EDTA), see Fig. S4(a), upon heating in order to transfer it into the gas phase, prevented experiments on dissociative electron attachment (DEA) to this compound. Therefore, we investigated methyliminodiacetic acid (MIDA), see Fig. S4. MIDA is basically one half of the EDTA molecule, see Fig. S4(b), with the other half replaced by a hydrogen atom, replacing the CH_2 group in the middle of the molecule depicted in Fig. S4(b) by a CH_3 group. Note that the molecule depicted in Fig. S4(b) corresponds to the dehydrogenated MIDA conformer, denoted here as M2, introduced below and depicted in Fig. S4. The same methods were used like for the TRIS calculations.

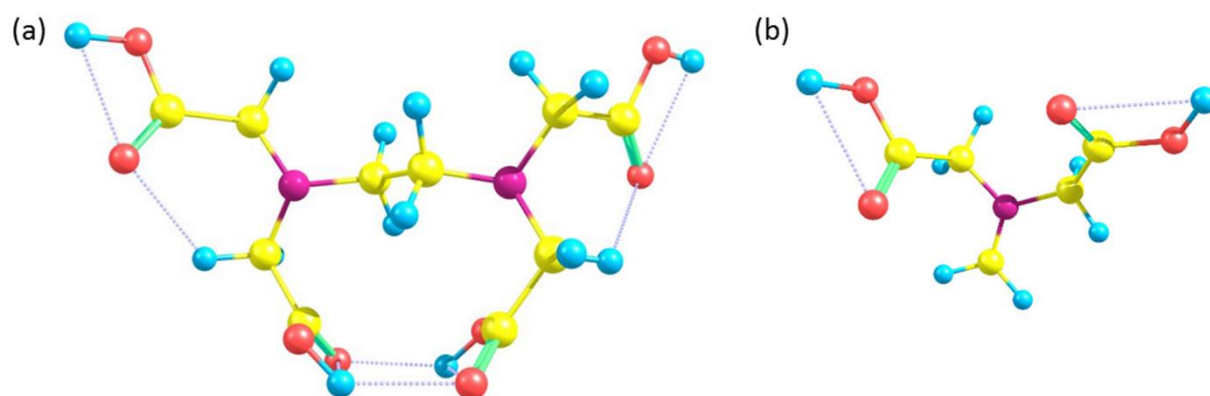


Figure S4: (a) EDTA. (b) Half of EDTA. Red: oxygen; purple: nitrogen; yellow: carbon; blue: hydrogen.

2.2.2. Results

2.2.2.1 Composition of the gas-phase sample at non-zero temperatures

We identified several local minimum configurations of MIDA, which are depicted in Fig. S5. In thermal equilibrium at zero temperature, $T=0$, MIDA would exist in the gas phase solely in its lowest energy conformeric form, which we find to be the M1 conformer, see Fig. S5. The conformers M2 to M7 yield higher energies than M1 by 0.04, 0.08, 0.22, 0.25, 0.30 and 0.53 eV, respectively. At non-

zero temperatures, however, a gas-phase sample of MIDA will be composed of a mixture of various conformeric forms. This composition can be estimated from the difference in (Gibbs) free energies between the different conformers, ΔG . The (Gibbs) free energy is given by $G=H-TS$, where $H=E+pV$ with E , p , V , T , S , H denoting the energy, pressure, volume, temperature, entropy and enthalpy of the molecular system, respectively. The ratio of concentrations in the sample of conformers $M1$ and $M2$, for instance, can be derived from the equilibrium constant $K_{12}=\exp(-\Delta G_{12}/k_B T)$, where k_B denotes the Boltzmann constant and the indices correspond to the involved conformers $M1$ and $M2$. In thermal equilibrium, the ratio of concentrations is given by K_{12} , i.e. $K_{12}=[M1]/[M2]$ (here the squared brackets indicate that concentrations are considered), assuming that the pressure is low enough such that $M1$ and $M2$ can be considered as ideal gases or, equivalently, such that the activity coefficients (linking the concentrations to activities) are close to unity. With these assumptions, we calculated the composition of a gas-phase sample of MIDA considering conformers $M1$ to $M7$ and using $[M1]+[M2]+\dots+[M7]=1$ in the temperature range $298.15\text{ K (room temperature)} < T < 450\text{ K}$, see Fig. S6. We find that the conformers $M1$, $M2$ and $M3$ dominate the composition with concentrations of 82.1, 13.7 and 4.2% at room temperature and 68.5, 20.8 and 10.4% at 450 K, respectively, over the considered temperature range. Due to this fact, we limited the calculation of thermochemical reaction thresholds for DEA to these three conformers. Before we proceed to the discussion of thermochemical reaction thresholds, we note that we calculated also (adiabatic) electron affinities (EAs) for the seven considered conformers of MIDA. We find that only two of the conformers yield stable valence bound anions (positive electron affinities). These are the $M1$ and the $M4$ conformers with (adiabatic) EAs of 0.20 and 0.27 eV, respectively. The two stable anions, $A1$ and $A2$, are also depicted in Fig. S5. We note that upon electron attachment to both $M1$ and $M4$, a hydrogen atom is transferred from one carboxyl group to the other. However, apart from the discussed valence bound anions, we note that also for some of the other conformers dipole-bound states might exist.

In order to investigate if and how our data could be transferred to the case of EDTA, we consider also the reaction energetics for a dehydrogenated version of the $M2$ conformer. In particular, one hydrogen atom is removed from the methyl group of this molecule. Then the resulting molecule corresponds to

half of the EDTA molecule. For this reason, the dehydrogenated M2 conformer will be denoted by E in the following.

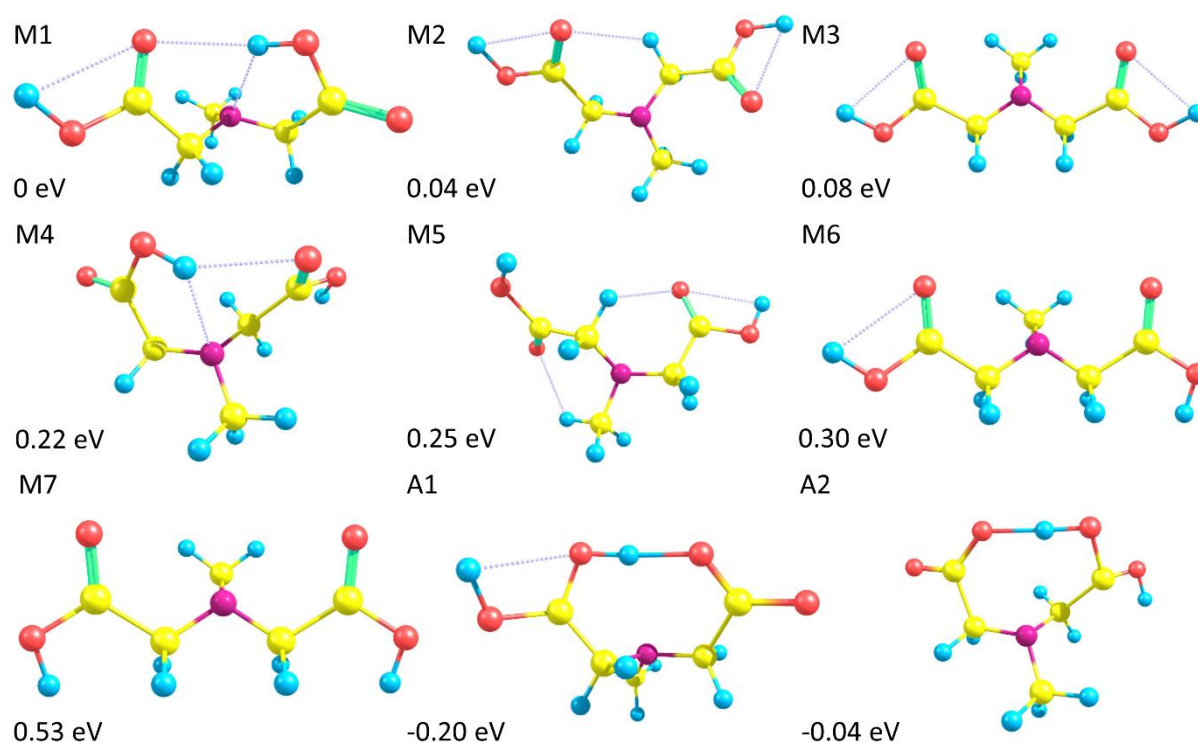


Figure S5: Various MIDA conformers (M1-M7) and two conformers of stable anions (A1 and A2). The given energies refer to the energy of the most stable MIDA conformer (M1) used as reference energy (i.e. 0 eV). Red: oxygen; purple: nitrogen; yellow: carbon; blue: hydrogen.

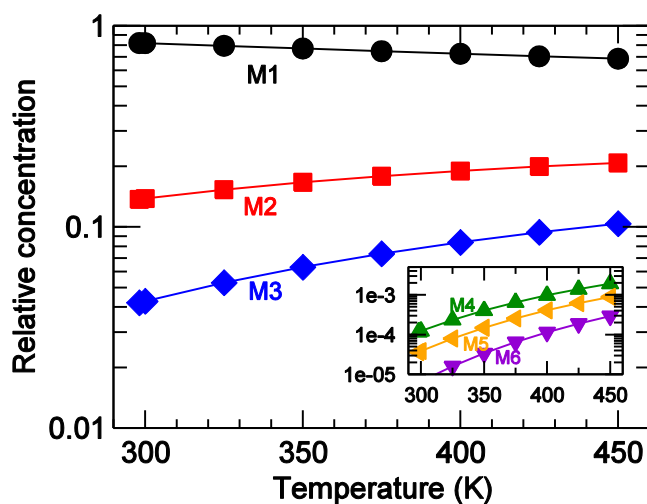


Figure S6: Relative concentrations of different MIDA conformers in a MIDA gas phase sample in thermal equilibrium. The concentration of M7 (not shown here) is lower than 10^{-5} for all considered temperatures.

2.2.2.2 Thermochemical reaction thresholds

In the following, we discuss the thermochemical reaction thresholds as obtained with G4(MP2) by evaluating the reaction (Gibbs) free energies at $T = 0, 298.15$ and 450 K and $p = 0$ bar for the considered fragmentation processes upon DEA to MIDA. The considered fragments are (MIDA-H)⁻, (MIDA-OH)⁻, (MIDA-COOH)⁻, (MIDA-HCOOH)⁻, (MIDA-CH₂COOH)⁻, COOH⁻ and OH⁻ with mass-to-charge ratios $m/z = 146, 130, 102, 101, 88, 45$ and 17 , as well as fragments with $m/z = 42$ which may be assigned to CNO⁻, CH₂CO⁻ or H₂CNCH₂⁻. We proceed from higher to lower m/z in the following.

2.2.2.2.1 (MIDA-H)⁻, $m/z=146$

The (Gibbs) free reaction energies for $T = 0, 298.15$ and 450 K and $p = 0$ bar for fragmentation reactions upon DEA involving (MIDA-H)⁻ fragments are summarized in Table S2. The corresponding fragments are depicted in Fig. S7. We note that the different conformers give rise to substantial differences in some of the respective reaction energies. The highly symmetrical M3 conformer of MIDA gives rise to reaction energies of $1.71, 0.74$ and 2.45 eV at room temperature ($=298.15$ K) for the abstraction of a hydrogen atom from the CH₂, COOH and CH₃ groups, respectively. Similar values can be found for reactions involving the two other conformers, i.e. M1 and M2. However, in addition to these values, we find also significant variations depending on the local geometrical configuration of the respective conformer and/or fragment. For instance, for the abstraction of the hydrogen atom from the CH₂ group close the carboxyl group in *trans* configuration (left carboxyl group of M1 in Fig. S5) we find a reaction threshold of 1.06 eV, which is significantly lower than the 1.73 eV found for the H abstraction from the CH₂ group close to the carboxyl group in *cis* configuration (which is a similar value as found for M3). For the H abstraction from the carboxyl group in *trans* configuration in M1, we find that this threshold becomes exothermic at elevated temperatures (450 K) yielding -0.12 eV. Such a dependence on molecular geometry is also apparent when the reaction thresholds are compared to the ones for the dehydrogenated M2 conformer (H abstraction from the methyl group) which

corresponds to one half of the EDTA molecule and is thus denoted by E in Table S2 and the following Tables. Both, reaction channels involving H abstraction from CH₂ and COOH yield significantly increased reaction energies compared to the ones found for M1, M2 and M3. Most interestingly, for H abstraction from the central CH₂ group (which corresponds to the methyl group in the M1, M2 and M3 conformers) no stable anionic fragment is found (non-positive EA of (E-H)⁻ with the hydrogen atom removed from the central CH₂ group) and thus, this reaction channel does not appear in Table S2.

Table S2: (Gibbs) free reaction energies for T = 0, 298.15, 450 K and p = 0 for reactions involving (MIDA-H)⁻ and (E-H)⁻ fragments.

Reaction	Reaction energy (eV)		
	0 K	298.15 K	450 K
e ⁻ + M1 →			
(M1-H) ⁻ + H; H from CH ₂ ; see Fig. S4(a)	1.34	1.06	0.89
(M1-H) ⁻ + H; H from CH ₂ ; see Fig. S4(b)	2.04	1.73	1.54
(M1-H) ⁻ + H; H from COOH; see Fig. S4(c)	0.30	0.04	-0.12
(M1-H) ⁻ + H; H from COOH; see Fig. S4(d)	0.99	0.70	0.52
(M1-H) ⁻ + H; H from CH ₃ ; see Fig. S4(e)	3.13	2.84	2.65
e ⁻ + M2 →			
(M2-H) ⁻ + H; H from CH ₂ ; see Fig. S4(f)	2.13	1.82	1.63
(M2-H) ⁻ + H; H from CH ₂ ; see Fig. S4(g)	2.02	1.73	1.53
(M2-H) ⁻ + H; H from COOH; see Fig. S4(h)	0.95	0.66	0.47
(M2-H) ⁻ + H; H from COOH; see Fig. S4(i)	1.13	0.81	0.62
(M2-H) ⁻ + H; H from CH ₃ ; see Fig. S4(j)	2.77	2.48	2.30
e ⁻ + M3 →			
(M3-H) ⁻ + H; H from CH ₂ ; see Fig. S4(k)	2.04	1.71	1.49
(M3-H) ⁻ + H; H from COOH; see Fig. S4(l)	1.05	0.74	0.55
(M3-H) ⁻ + H; H from CH ₃ ; see Fig. S4(m)	2.73	2.45	2.27
e ⁻ + E →			
(E-H) ⁻ + H; H from CH ₂ ; see Fig. S4(n)	2.39	2.17	
(E-H) ⁻ + H; H from CH ₂ ; see Fig. S4(o)	2.39	2.14	
(E-H) ⁻ + H; H from COOH; see Fig. S4(p)	2.79	2.54	
(E-H) ⁻ + H; H from COOH; see Fig. S4(q)	1.50	1.29	

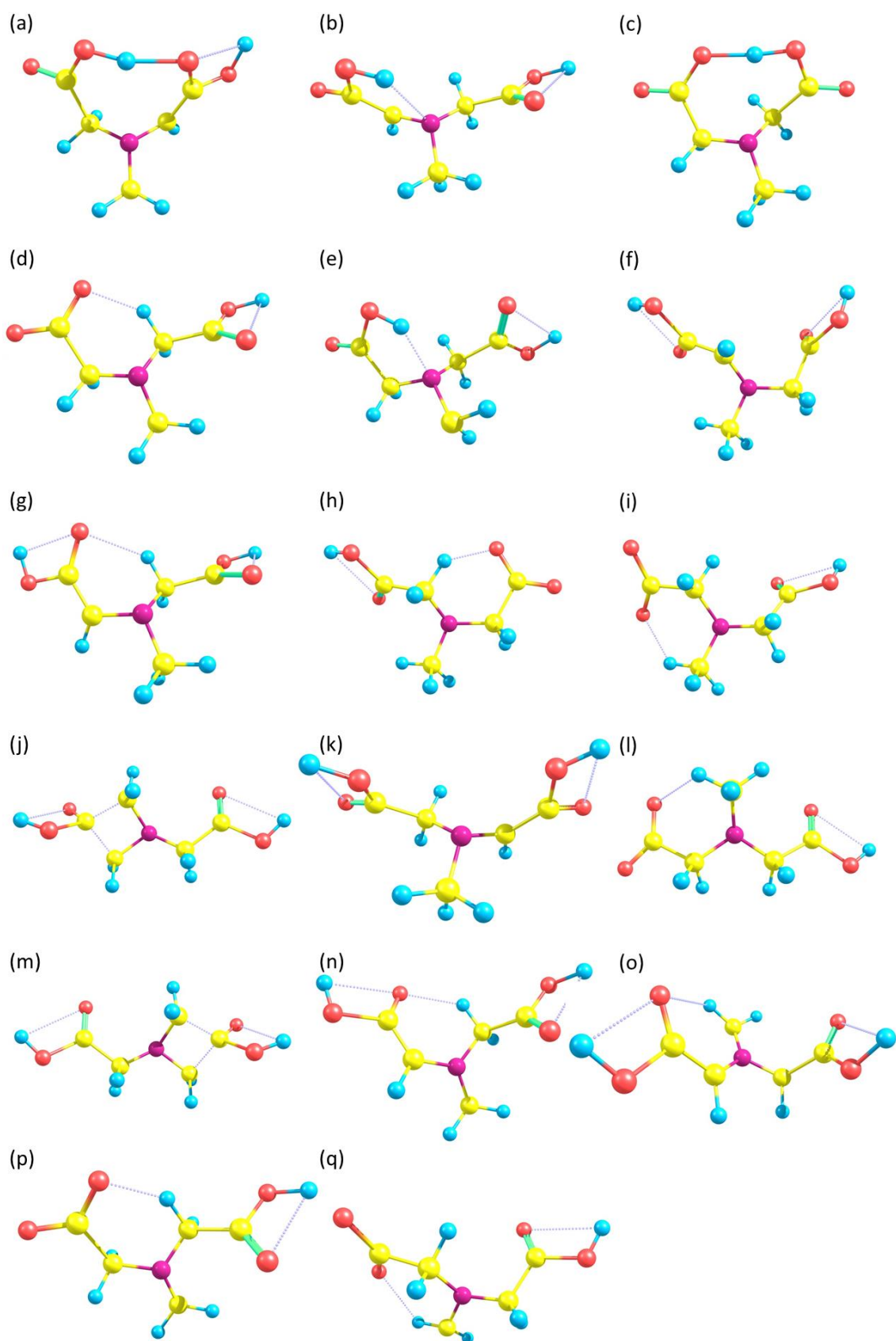


Figure S7: (MIDA-H)⁻ and (E-H)⁻ fragments appearing in Table S2. Red: oxygen; purple: nitrogen; yellow: carbon; blue: hydrogen.

2.2.2.2.2 (MIDA-OH)⁻, m/z=130

As already noted in section 2.2.2.2.1, we observe also in the case of (MIDA-OH)⁻ fragments a dependence of the threshold energies on the local molecular geometry, see Table S3. So yields the abstraction of the OH radical from the carboxyl group in *trans* configuration a threshold which is about 0.5 eV lower than the thresholds from abstraction of OH from the carboxyl groups in *cis* configuration. The latter yield rather similar values for the different conformers, although we note that there exist also different conformers of the resulting anions which slightly affect the reaction energetics (see the two reaction channels for the M2 conformer). Probably most interesting is the fact, that (E-OH) yields no stable anion and thus there appears no reaction channel for E in Table 3, i.e. the formation of (E-OH)⁻ and an OH radical is not possible via DEA to E in strong contrast to MIDA. Structures of the fragments appearing in Table S3 are depicted in Fig. S8.

Table S3: (Gibbs) free reaction energies for T = 0, 298.15, 450 K and p = 0 for reactions involving (MIDA-OH)⁻ fragments.

Reaction	Reaction energy (eV)		
	0 K	298.15 K	450 K
e ⁻ + M1 →			
(M1-OH) ⁻ + OH; see Fig. S5(a)	3.84	3.42	3.16
(M1-OH) ⁻ + OH; see Fig. S5(b)	3.34	2.93	2.70
e ⁻ + M2 →	0 K	298.15 K	450 K
(M2-OH) ⁻ + OH; see Fig. S5(c)	3.83	3.40	3.15
(M2-OH) ⁻ + OH; see Fig. S5(d)	3.96	3.51	3.23
e ⁻ + M3 →	0 K	298.15 K	450 K
(M3-OH) ⁻ + OH; see Fig. S5(e)	3.88	3.42	3.15

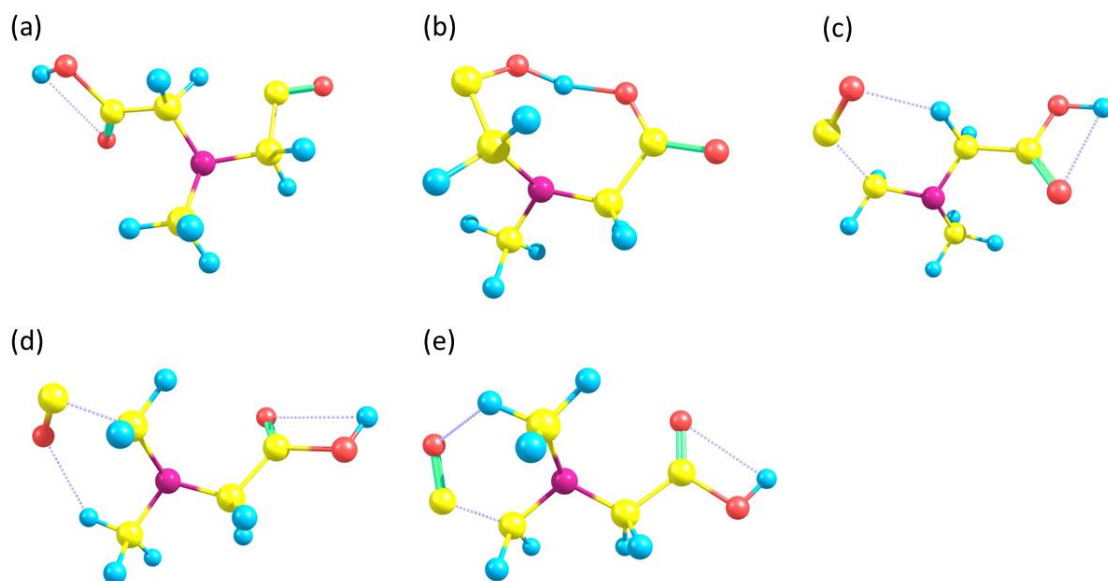


Figure S8: (MIDA-OH)⁻ fragments appearing in Table S2. Red: oxygen; purple: nitrogen; yellow: carbon; blue: hydrogen.

2.2.2.2.3 (M-COOH)⁻, m/z=102

The (Gibbs) free reaction energies for $T = 0, 298.15$ and 450 K and $p = 0$ bar for fragmentation reactions upon DEA involving (MIDA-COOH)⁻ fragments are summarized in Table S4. The fragments appearing in Table S4 are depicted in Fig. S9. Apart from another apparent difference between *cis* and *trans* carboxyl groups concerning the M1, M2 and M3 conformers, we note that taking into account only the total energy balance, the loss of COOH appears possible at considerably lower energies (lower by about 1 eV) for the E molecule, i.e. the dehydrogenated M3 conformer (H abstraction from CH₃ group) than for the MIDA conformers.

It is also important to note at this point that there exist two energetically slightly distinct conformers of COOH, i.e. the *cis* and *trans* variant of this radical, see Fig. S9(g) and (h), respectively. Using G4(MP2) we obtain for these conformers an energy difference (at $T = 0$ K) of about 0.07 eV favoring the *trans* configuration in good agreement with the literature (3). In Table S4, we have listed only those reaction channels in which the geometry of the carboxyl radical has not changed from the geometry of the carboxyl group in the molecule (before fragmentation). Actually, for each of the listed

reaction channels, there exists also a channel taking into account a possible transition of the carboxyl fragment from its respective conformeric form to the other.

Table S4: (Gibbs) free reaction energies for $T = 0, 298.15, 450$ K and $p = 0$ for reactions involving $(\text{MIDA-COOH})^-$ and $(\text{E-COOH})^-$ fragments.

Reaction	Reaction energy (eV)		
	0 K	298.15 K	450 K
$e^- + \text{M1} \rightarrow$			
$(\text{M1-COOH})^- + \text{cis-COOH}$; see Fig. S6(a)	3.37	2.83	2.54
$(\text{M1-COOH})^- + \text{trans-COOH}$; see Fig. S6(b)	2.54	2.00	1.71
$e^- + \text{M2} \rightarrow$			
$(\text{M2-COOH})^- + \text{cis-COOH}$; see Fig. S6(c)	3.49	2.95	2.65
$(\text{M2-COOH})^- + \text{cis-COOH}$; see Fig. S6(d)	3.40	2.86	2.56
$e^- + \text{M3} \rightarrow$			
$(\text{M3-COOH})^- + \text{cis-COOH}$; see Fig. S6(e)	3.41	2.85	2.54
$e^- + \text{E} \rightarrow$			
$(\text{E-COOH})^- + \text{cis-COOH}$; see Fig. S6(f)	2.36	1.87	

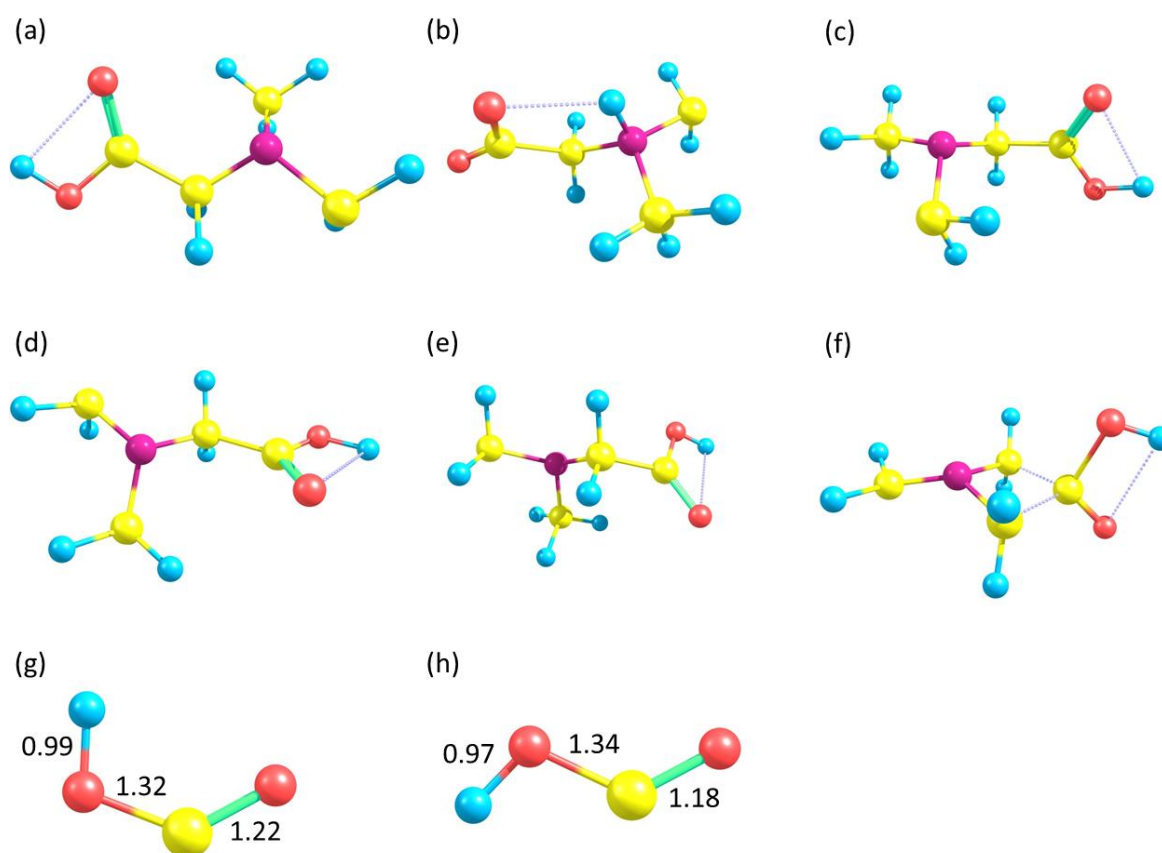


Figure S9: (a)-(f): $(\text{MIDA-COOH})^-$ and $(\text{E-COOH})^-$ fragments appearing in Table S4. (g) and (h): Structures of neutral *cis*-COOH and *trans*-COOH fragments with bond lengths in Å. Red: oxygen; purple: nitrogen; yellow: carbon; blue: hydrogen.

2.2.2.2.4 (M-HCOOH)⁻, m/z=101

The (Gibbs) free reaction energies for $T = 0, 298.15$ and 450 K and $p = 0$ bar for fragmentation reactions upon DEA involving (MIDA-HCOOH)⁻ fragments are summarized in Table S5. The structures of the corresponding fragments are depicted in Fig. S10. As for the previous case of carboxyl loss, also for the formation of formic acid (HCOOH), there exist complications due to two conformers of formic acid, i.e. *cis* and *trans* configurations of formic acid. This time, in Table S5, each reaction channel appears twice: once giving rise to *cis*-HCOOH, once to *trans*-HCOOH. The two conformers are separated by 0.17 eV according to G4(MP2), which yields good agreement with the literature ($1365\text{ cm}^{-1} \approx 0.17\text{ eV}$).⁽⁴⁾ The barrier for *cis*→*trans* conversion is about 0.35 eV according to the literature.⁽⁵⁾ We note that exothermic formation of formic acid upon DEA to MIDA, but also to E (half of EDTA), appears possible via many channels, but involves the transfer of a hydrogen atom to one of the carboxyl groups in the respective molecule. We noted already above for M1, that its anion (A1) yields such a transfer of a hydrogen atom from the other carboxyl group. However, using only the thermochemical data listed in Table S5 other pathways including hydrogen transfer from other groups (CH₂, CH₃) cannot be excluded. However, some pathways can be easily excluded by noting the instability of certain fragment anions. For example, abstraction of a hydrogen atom from the methyl group and concurrent abstraction of the carboxyl group from the M3 conformer results in a fragment which yields a non-positive EA. So it can be concluded that the formation of formic acid and the (MIDA-HCOOH)⁻ fragment cannot proceed via hydrogen transfer from the methyl group considering the M3 conformer of MIDA. The very same is the case for several other anionic fragments which are thus not listed in Table S5.

Furthermore, we note that the energy required to break the C-H bond in *trans*-HCOOH is obtained as 4.16 eV. Hence, the reaction $e^- + M \rightarrow (M\text{-HCOOH})^- + H + \text{COOH}$ is endothermic. Formation of (M-HCOOH)⁻ is thus probably only possible with zero-energy electrons via formation of formic acid.

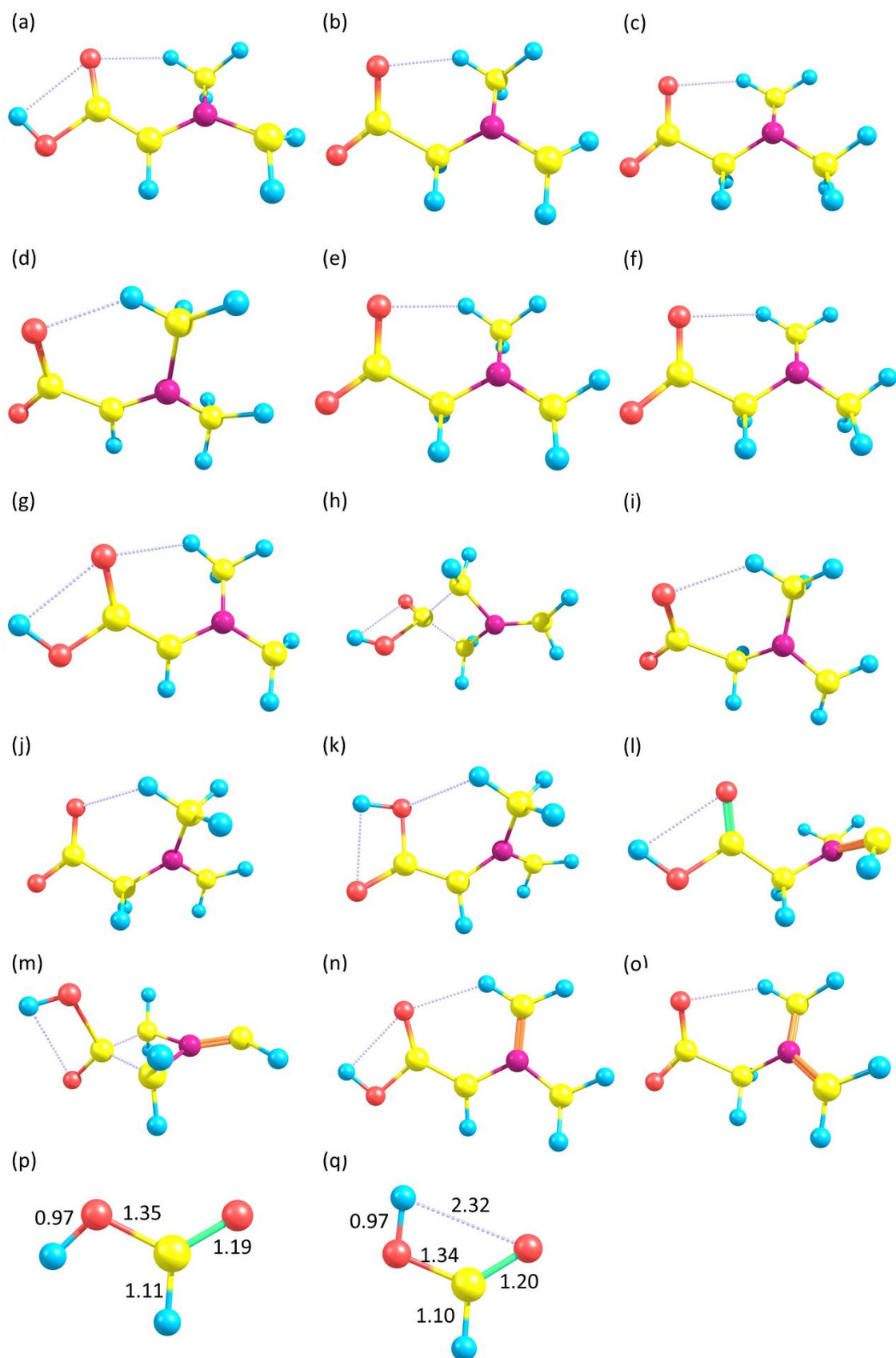


Figure S10: (a)-(o): (MIDA-HCOOH)⁻ and (E-HCOOH)⁻ fragments appearing in Table S5. (p) and (q): Structures of neutral *cis*-HCOOH and *trans*-HCOOH fragments with bond lengths in Å. Red: oxygen; purple: nitrogen; yellow: carbon; blue: hydrogen.

Table S5: (Gibbs) free reaction energies for T = 0, 298.15, 450 K and p = 0 for reactions involving (MIDA-HCOOH)⁻ fragments.

Reaction	Reaction energy (eV)		
	0 K	298.15 K	450 K
$e^- + M1 \rightarrow$			
(M1-HCOOH) ⁻ + <i>cis</i> -HCOOH; see Fig. S7(a)	1.41	0.86	0.56
(M1-HCOOH) ⁻ + <i>trans</i> -HCOOH; see Fig. S7(a)	1.25	0.70	0.39
(M1-HCOOH) ⁻ + <i>cis</i> -HCOOH; see Fig. S7(b)	0.49	-0.08	-0.40
(M1-HCOOH) ⁻ + <i>trans</i> -HCOOH; see Fig. S7(b)	0.32	-0.25	-0.56
(M1-HCOOH) ⁻ + <i>cis</i> -HCOOH; see Fig. S7(c)	0.58	0.02	-0.28
(M1-HCOOH) ⁻ + <i>trans</i> -HCOOH; see Fig. S7(c)	0.41	-0.15	-0.45
(M1-HCOOH) ⁻ + <i>cis</i> -HCOOH; see Fig. S7(d)	0.46	-0.08	-0.38
(M1-HCOOH) ⁻ + <i>trans</i> -HCOOH; see Fig. S7(d)	0.30	-0.25	-0.51
(M1-HCOOH) ⁻ + <i>cis</i> -HCOOH; see Fig. S7(e)	0.45	-0.11	-0.41
(M1-HCOOH) ⁻ + <i>trans</i> -HCOOH; see Fig. S7(e)	0.28	-0.27	-0.57
(M1-HCOOH) ⁻ + <i>cis</i> -HCOOH; see Fig. S7(f)	0.58	0.02	-0.28
(M1-HCOOH) ⁻ + <i>trans</i> -HCOOH; see Fig. S7(f)	0.41	-0.15	-0.45
$e^- + M2 \rightarrow$	0 K	298.15 K	450 K
(M2-HCOOH) ⁻ + <i>cis</i> -HCOOH; see Fig. S7(g)	1.37	0.82	0.51
(M2-HCOOH) ⁻ + <i>trans</i> -HCOOH; see Fig. S7(g)	1.20	0.65	0.35
(M2-HCOOH) ⁻ + <i>cis</i> -HCOOH; see Fig. S7(h)	2.11	1.59	1.31
(M2-HCOOH) ⁻ + <i>trans</i> -HCOOH; see Fig. S7(h)	1.95	1.42	1.14
(M2-HCOOH) ⁻ + <i>cis</i> -HCOOH; see Fig. S7(i)	0.44	-0.13	-0.44
(M2-HCOOH) ⁻ + <i>trans</i> -HCOOH; see Fig. S7(i)	0.28	-0.29	-0.61
$e^- + M3 \rightarrow$	0 K	298.15 K	450 K
(M-HCOOH) ⁻ + <i>cis</i> -HCOOH; see Fig. S7(j)	0.41	-0.16	-0.47
(M-HCOOH) ⁻ + <i>trans</i> -HCOOH; see Fig. S7(j)	0.24	-0.32	-0.64
(M-HCOOH) ⁻ + <i>cis</i> -HCOOH; see Fig. S7(k)	1.40	0.86	0.56
(M-HCOOH) ⁻ + <i>trans</i> -HCOOH; see Fig. S7(k)	1.24	0.69	0.40
$e^- + E \rightarrow$	0 K	298.15 K	450 K
(E-HCOOH) ⁻ + <i>cis</i> -HCOOH; see Fig. S7(l)	1.82	1.33	
(E-HCOOH) ⁻ + <i>trans</i> -	1.65	1.16	

HCOOH; see Fig. S7(l) (E-HCOOH) ⁻ + <i>cis</i> - HCOOH; see Fig. S7(m)	1.06	0.60
(E-HCOOH) ⁻ + <i>trans</i> - HCOOH; see Fig. S7(m)	0.89	0.43
(E-HCOOH) ⁻ + <i>cis</i> - HCOOH; see Fig. S7(n)	0.23	-0.23
(E-HCOOH) ⁻ + <i>trans</i> - HCOOH; see Fig. S7(n)	0.06	-0.40
(E-HCOOH) ⁻ + <i>cis</i> - HCOOH; see Fig. S7(o)	-0.55	-1.05
(E-HCOOH) ⁻ + <i>trans</i> - HCOOH; see Fig. S7(o)	-0.72	-1.22

2.2.2.2.5 (M-CH₂COOH)⁻, m/z=88

The (Gibbs) free reaction energies for T = 0, 298.15 and 450 K and p = 0 bar for fragmentation reactions upon DEA involving (MIDA-CH₂COOH)⁻ fragments are summarized in Table S6. Structures of the corresponding fragments are depicted in Fig. S11. Similarly to other already discussed fragmentation channels, we observe also here a significant difference due to *cis* and *trans* configurations present in the M1 conformer. Whereas formation of the (MIDA-CH₂COOH)⁻ fragment exhibiting a carboxyl group in *trans* configuration and a neutral CH₂COOH fragment is endothermic (and yields similar reaction thresholds for all MIDA conformers under consideration), the loss of the *trans*-CH₂COOH is exothermic. We also note that the (E-CH₂COOH) fragment yields a non-positive EA and thus no stable valence bound anion exists, again in strong contrast to the MIDA conformers.

Table S6: (Gibbs) free reaction energies for T = 0, 298.15, 450 K and p = 0 for reactions involving (MIDA-CH₂COOH)⁻ fragments.

Reaction	Reaction energy (eV)		
	0 K	298.15 K	450 K
e ⁻ + M1 →			
(M1-CH ₂ COOH) ⁻ + <i>cis</i> -CH ₂ COOH; see Figs. S8(a) and (e)	2.24	1.69	1.39
(M1-CH ₂ COOH) ⁻ + <i>trans</i> -CH ₂ COOH; see Figs. S8(a) and (f)	2.03	1.49	1.19
(M1-CH ₂ COOH) ⁻ + <i>cis</i> -CH ₂ COOH; see Figs. S8(b) and (e)	0.39	-0.17	-0.48
(M1-CH ₂ COOH) ⁻ + <i>trans</i> -CH ₂ COOH; see Figs. S8(b) and (f)	0.19	-0.37	-0.67
e ⁻ + M2 →			
(M2-CH ₂ COOH) ⁻ + <i>cis</i> -CH ₂ COOH; see	2.27	1.68	1.36

Figs. S8(c) and (e) (M2-CH ₂ COOH) ⁻ + <i>trans</i> -CH ₂ COOH; see Figs. S8(c) and (f)	2.06	1.48	1.17
e ⁻ + M3 →	0 K	298.15 K	450 K
(M-CH ₂ COOH) ⁻ + <i>cis</i> - CH ₂ COOH; see Figs. S8(d) and (e)	2.23	1.65	1.33
(M-CH ₂ COOH) ⁻ + <i>trans</i> -CH ₂ COOH; see Figs. S8(d) and (f)	2.02	1.45	1.14

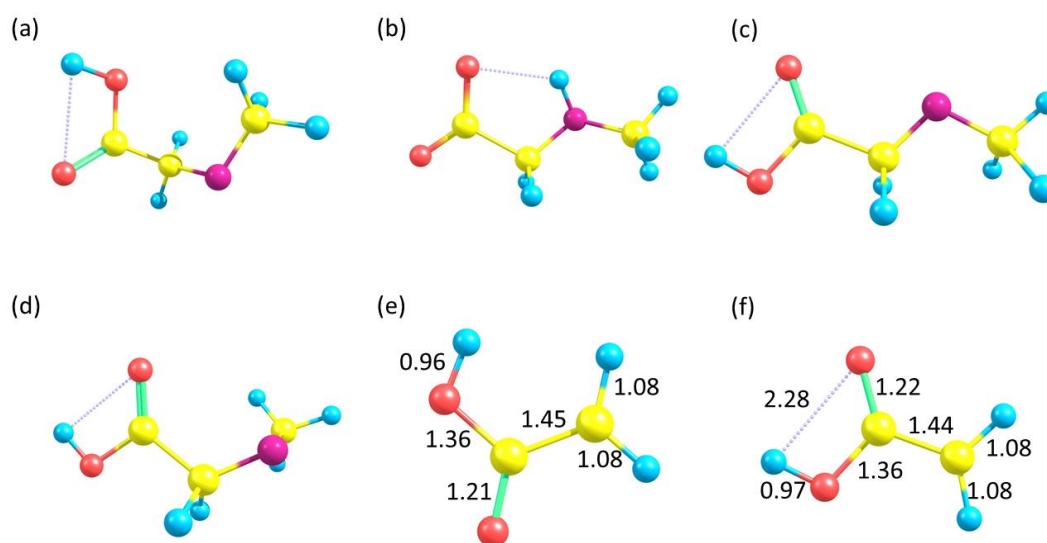


Figure S11: (a)-(d): (MIDA-CH₂COOH)⁻ fragments appearing in Table S6. (p) and (q): Structures of neutral *cis*-CH₂COOH and *trans*-CH₂COOH fragments with bond lengths in Å. Red: oxygen; purple: nitrogen; yellow: carbon; blue: hydrogen.

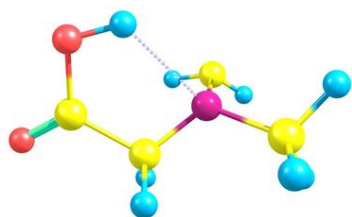
2.2.2.2.6 COOH⁻, m/z=45

The (Gibbs) free reaction energies for T = 0, 298.15 and 450 K and p = 0 bar for fragmentation reactions upon DEA involving COOH⁻ fragments are summarized in Table S7. The corresponding fragment structures are depicted in Fig. S12. The energy difference between *cis* and *trans* conformers of the carboxyl anions was obtained as 0.06 eV, this time the *cis*-conformer is more stable. Splitting of reaction channels due to possible transitions has not been taken into account in Table S7.

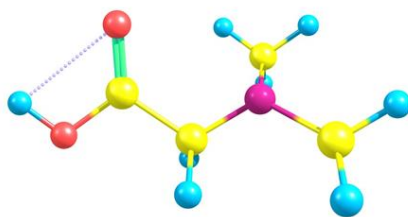
Table S7: (Gibbs) free reaction energies for T = 0, 298.15, 450 K and p = 0 for reactions involving COOH⁻ fragments.

Reaction	Reaction energy (eV)		
	0 K	298.15 K	450 K
$e^- + M1 \rightarrow$			
(M1-COOH) + <i>cis</i> -COOH; see Figs. S9(a) and (g)	1.96	1.40	1.08
(M1-COOH) + <i>trans</i> -COOH; see Figs. S9(b) and (h)	2.06	1.50	1.18
$e^- + M2 \rightarrow$			
(M2-COOH) + <i>cis</i> -COOH; see Figs. S9(c) and (g)	1.97	1.39	1.06
(M2-COOH) ⁻ + <i>cis</i> -COOH; see Figs. S9(d) and (g)	1.92	1.35	1.04
$e^- + M3 \rightarrow$			
(M3-COOH) + <i>cis</i> -COOH; see Figs. S9(e) and (g)	1.88	1.32	1.01
$e^- + E \rightarrow$			
(E-COOH) + <i>cis</i> -COOH; see Figs. S9(f) and (g)	1.05	0.54	

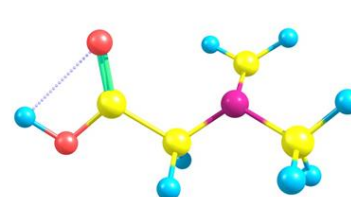
(a)



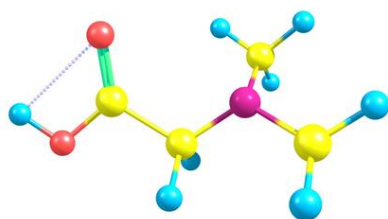
(b)



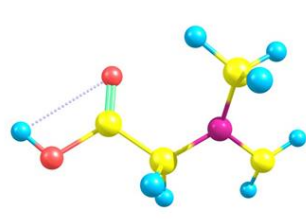
(c)



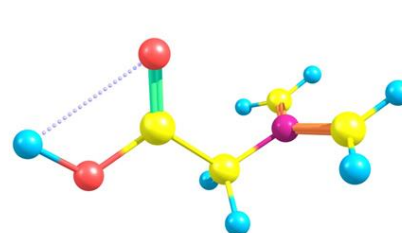
(d)



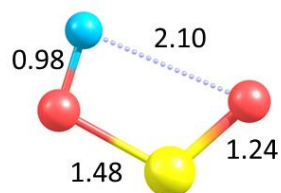
(e)



(f)



(g)



(h)

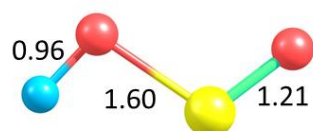


Figure S12: (a)-(f): (MIDA-COOH) and (E-COOH) fragments appearing in Table S6. (g) and (h): Structures of *cis*-COOH and *trans*-COOH anions with bond lengths in Å. Red: oxygen; purple: nitrogen; yellow: carbon; blue: hydrogen.

2.2.2.2.7 $m/z=42$

Concerning DEA to MIDA, one can think of (at least) three possible anions with $m/z=42$: CNO^- , CH_2CO^- , $\text{H}_2\text{CNCH}_2^-$. However, CH_2CO yields a non-positive EA, so it was excluded. CNO^- yields reaction energies above 13 eV. Most probable appear thus reaction channels involving the fragment $\text{H}_2\text{CNCH}_2^-$. Possible reaction channels and reaction energies are listed in Table S8. The optimized structure of $\text{H}_2\text{CNCH}_2^-$ is depicted in Fig. S13(a).

Table S8: (Gibbs) free reaction energies for $T = 0, 298.15, 450 \text{ K}$ and $p = 0$ for reactions involving $\text{H}_2\text{CNCH}_2^-$ fragments.

Reaction	Reaction energy (eV)		
	0 K	298.15 K	450 K
$e^- + \text{M1} \rightarrow$			
$\text{H}_2\text{CNCH}_2^- + \text{CH}_3 + \text{cis-HCOOH} + \text{CO}_2$	2.99	1.49	0.65
$\text{H}_2\text{CNCH}_2^- + \text{CH}_3 + \text{trans-HCOOH} + \text{CO}_2$	2.82	1.33	0.49
$e^- + \text{M2} \rightarrow$			
$\text{H}_2\text{CNCH}_2^- + \text{CH}_3 + \text{cis-HCOOH} + \text{CO}_2$	2.95	1.45	0.60
$\text{H}_2\text{CNCH}_2^- + \text{CH}_3 + \text{trans-HCOOH} + \text{CO}_2$	2.78	1.28	0.44
$e^- + \text{M3} \rightarrow$			
$\text{H}_2\text{CNCH}_2^- + \text{CH}_3 + \text{cis-HCOOH} + \text{CO}_2$	2.91	1.42	0.58
$\text{H}_2\text{CNCH}_2^- + \text{CH}_3 + \text{trans-HCOOH} + \text{CO}_2$	2.74	1.25	0.41
$e^- + \text{E} \rightarrow$			
$\text{H}_2\text{CNCH}_2^- + \text{CH}_2 + \text{cis-HCOOH} + \text{CO}_2$	3.88	2.45	
$\text{H}_2\text{CNCH}_2^- + \text{CH}_2 + \text{trans-HCOOH} + \text{CO}_2$	3.71	2.28	

2.2.2.2.8 OH^- , $m/z=17$

The (Gibbs) free reaction energies for $T = 0, 298.15$ and 450 K and $p = 0$ bar for fragmentation reactions upon DEA involving OH^- fragments are summarized in Table S8. The corresponding fragments are depicted in Fig. S13. Very similar results were obtained for the three considered conformers of MIDA. Again, there is a substantial difference for E (half of EDTA) compared to

MIDA, i.e. the respective reaction threshold is about 1 eV lower than the ones obtained for the MIDA conformers M1, M2 and M3.

Table S9: (Gibbs) free reaction energies for $T = 0, 298.15, 450$ K and $p = 0$ for reactions involving OH⁻ fragments.

Reaction	Reaction energy (eV)		
	0 K	298.15 K	450 K
$e^- + M1 \rightarrow$ (M1-OH) from cis + OH ⁻	2.59	2.15	1.88
(M1-OH) from trans + OH ⁻	2.58	2.15	1.90
$e^- + M2 \rightarrow$ (M2-OH) + OH ⁻	2.56	2.12	1.86
$e^- + M3 \rightarrow$ (M3-OH) + OH ⁻	2.56	2.11	1.85
$e^- + E \rightarrow$ (E-OH-CO) + CO + OH ⁻	1.56	1.06	

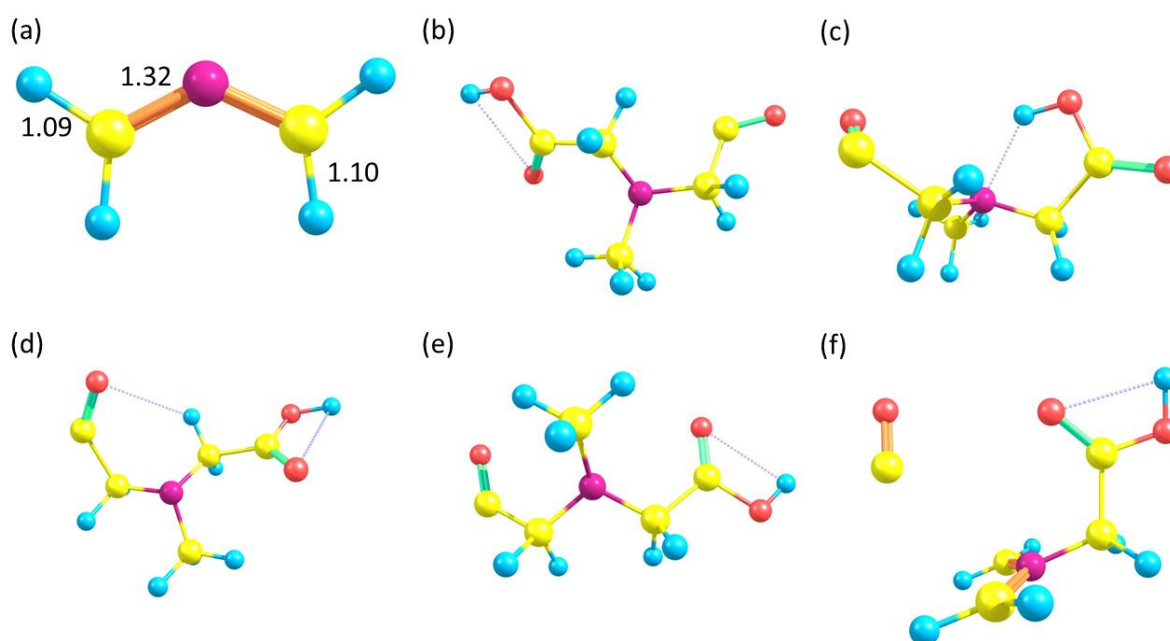


Figure S13: (a): Optimized structure of $H_2CNCH_2^-$ appearing in Table S8. (b)-(f): (MIDA-OH) and (E-OH-CO) fragments appearing in Table S9. Red: oxygen; purple: nitrogen; yellow: carbon; blue: hydrogen.

2.2.2. Summary and concluding remarks

Thermochemical reaction thresholds were calculated for the three most stable identified conformers of MIDA which are also dominantly abundant in a temperature range from room temperature to 450 K (the other conformers account together for less than 1% at all considered temperatures). Several

exothermic fragmentation reactions upon DEA were found including the reaction channels resulting in the formation of formic acid and (MIDA-HCOOH)⁻, as well as formation of the fragments (MIDA-CH₂COOH)⁻ and CH₂COOH. The molecular geometry was found to play an important role in order to explain differences in the total energy balance concerning various reaction channels. A variety of different conformers also for neutral and anionic fragments gives rise to many subtleties which might require further elaboration. Exploration of parts of the potential energy surfaces for the three conformers M1, M2 and M3 may be required to clarify from which part of the molecule a hydrogen atom may be transferred to a carboxyl group already at zero energy in order to form formic acid. Nevertheless, already the investigation of the thermochemical energy balance for the various fragmentation channels is sufficient to conclude that the results obtained for MIDA cannot be straightforwardly transferred to the case of dehydrogenated MIDA or half of EDTA. MIDA might be rather seen as a model for EDTA itself. The replacement of one half of EDTA by a hydrogen atom does possibly not affect the local electronic structure. In contrast, abstraction of the hydrogen from the methyl group at least affects the bonding character of the respective carbon atom by inducing a change from sp³ to sp² hybridization.

Acknowledgement SI

The computational results presented have been achieved (in part) using the HPC infrastructure LEO of the University of Innsbruck. S.E.H gratefully acknowledges Dr. Andreas Mauracher for a thorough reading of this supporting information and highly adjuvant feedback on it.

References SI

1. Curtiss, L. A.; Redfern, P. C.; Raghavachari, K. Gaussian-4 theory using reduced order perturbation theory. *The Journal of Chemical Physics* **2007**, *127*, 124105.
2. Frisch, M. J.; Trucks, G. W.; Schlegel, H. B.; Scuseria, G. E.; Robb, M. A.; Cheese man, J. R.; Scalmani, G.; Barone, V.; Mennucci, B.; Petersson, G. A. et al. Gaussian 09 Revision C. Gaussian Inc. Wallingford CT 2009.

3. Aoyagi, M.; Kato, S. A theoretical study of the potential energy surface for the reaction $\text{OH} + \text{CO} \rightarrow \text{CO}_2 + \text{H}$. *The Journal of Chemical Physics* **1988**, 88, 6409-6418.
4. Pettersson, M.; Macoas, E.M.S.; Khriachtchev, L.; Lundell, J.; Fausto, R.; Rasanen, M. Cis \rightarrow trans conversion of formic acid by dissipative tunneling in solid rare gases: Influence of environment on the tunneling rate. *The Journal of Chemical Physics* **2002**, 117, 9095-9098.